

Quorum-sensing antiactivator TraM forms a dimer that dissociates to inhibit TraR

Guozhou Chen, James W. Malenkos, Mee-Rye Cha, Clay Fuqua and Lingling Chen*

Department of Biology, Indiana University, 915 E. 3rd St., Bloomington, IN 47405, USA.

Summary

The quorum-sensing transcriptional activator TraR of *Agrobacterium tumefaciens*, which controls the replication and conjugal transfer of the tumour-inducing (Ti) virulence plasmid, is inhibited by the TraM anti-activator. The crystal structure of TraM reveals this protein to form a homodimer in which the monomer primarily consists of two long coiled α -helices, and one of the helices from each monomer also bundles to form the dimeric interface. The importance of dimerization is addressed by mutational studies in which disruption of the hydrophobic dimer interface leads to aggregation of TraM. Biochemical studies confirm that TraM exists as a homodimer in solution in equilibrium with the monomeric form, and also establish that the TraM–TraR complex is a heterodimer. Thus, the TraM homodimer undergoes dissociation in forming the antiactivation complex. Combined with the structure of TraR (Zhang *et al.*, 2002, *Nature* 417: 971–974; Vannini *et al.*, 2002, *EMBO J* 21: 4393–4401), our structural analysis suggests overlapping interactive surfaces in homodimeric TraM with those in the TraM–TraR complex and a mechanism for TraM inhibition on TraR.

Introduction

Bacteria are capable of distributive behaviours via production and response to diffusible signal molecules. A significant number of these communication systems enable bacteria to monitor their population density in a process generally described as quorum sensing. In quorum sensing, molecular signal concentrations reflect the bacterial population density and, at a threshold level, or quorum, activate specific bacterial behaviours (Dunny and Winans, 1999; Miller and Bassler, 2001). Among members of the

large Proteobacteria group, a relatively common form of quorum sensing relies on synthesis and release of acylated homoserine lactones (AHLs; for reviews, see Fuqua and Greenberg, 2002; Williams, 2002). AHL-based quorum-sensing systems have garnered significant interest because of their frequent role in microbial virulence mechanisms and are considered to be important potential antimicrobial therapeutic targets (Parsek and Greenberg, 2000; Williams, 2002). A general model for AHL quorum sensing has emerged, based originally on the study of bioluminescence in marine *Vibrio* species and augmented more recently by work on other quorum-sensing bacteria. AHLs are usually synthesized by members of the LuxI family of proteins and released through the cytoplasmic membrane via passive diffusion or assisted by membrane transporters. In most environments, basal level AHL synthesis by a single cell is insufficient to activate the system; at higher population densities, the contribution of multiple AHL-producing cells leads to inducing levels of the signal molecules. Increased AHL concentration usually drives interaction with intracellular AHL receptors that are members of the LuxR family of transcription factors. In most cases, LuxR-type proteins complexed with AHLs bind to regulatory DNA elements called *lux*-type boxes, \approx 18–20 bp palindromes often centred at -42 , just upstream of the -35 region consensus sequence of target gene promoters. After binding to these *lux*-type boxes, LuxR-type proteins presumably recruit RNA polymerase for transcriptional initiation of target genes.

One of the best studied AHL quorum-sensing systems regulates the copy number and conjugation of the Ti (tumour-inducing) virulence plasmid from the plant pathogen *Agrobacterium tumefaciens* (Zhu and Winans, 1999). The *A. tumefaciens* AHL is 3-oxo-octanoyl-L-homoserine lactone (3-oxo-C8-HSL) synthesized by the TraI AHL synthase (Zhang *et al.*, 1993; Fuqua and Winans, 1994; Hwang *et al.*, 1994; Moré *et al.*, 1996). The TraR protein is an AHL-responsive LuxR-type transcription factor that activates genes controlling Ti plasmid replication (*rep*) and conjugal transfer (*tra*). In the absence of AHL or at low concentrations of the ligand, TraR is monomeric and subjected to rapid proteolysis (Zhu and Winans, 2001). At inducing concentrations, the AHL is bound by TraR, causing the formation of a stable, active homodimer with one AHL bound per TraR protomer. Dimerized TraR–AHL has an increased affinity for the control (*tra*-box) sequences

Accepted 3 March, 2004. *For correspondence. E-mail lingling@bio.indiana.edu; Tel. (+1) 812 855 0491; Fax (+1) 812 855 6082.

We dedicate this paper in memory of Felix Chen.

upstream of target *rep* and *tra* operons, resulting in binding of the DNA and, in turn, transcriptional activation (Fuqua *et al.*, 1996; Zhu and Winans, 1999; 2001; Luo *et al.*, 2000). As with other LuxR-type proteins, TraR is composed of two functionally distinct domains (Fuqua and Greenberg, 2002): an N-terminal AHL-binding domain that can promote dimerization of TraR (Chai *et al.*, 2001); and a C-terminal DNA-binding domain independently capable of activating target gene expression (Choi and Greenberg, 1991). Structural studies also reveal that these two domains are bridged via a flexible linker region, and the dimeric interface, the major contribution of which comes from the N-terminal domain, is largely hydrophobic in nature (Vannini *et al.*, 2002; Zhang *et al.*, 2002).

Two proteins function independently to inhibit TraR activity. One of these, called TrIR, is highly similar to TraR and truncated at its carboxyl-terminus, deleting the DNA-binding domain (Oger *et al.*, 1998; Zhu and Winans, 1998). In the presence of AHL, TrIR forms inactive heterodimers with TraR (Chai *et al.*, 2001). The other inhibitory protein is TraM (Fuqua *et al.*, 1995; Hwang *et al.*, 1995). TraM is a novel regulator that is conserved in several bacteria within the Rhizobiaceae family. The TraM protein exerts its antagonistic function, at least in part, through direct interaction with the DNA-binding domain of TraR (Luo *et al.*, 2000). The TraM–TraR complex is very stable with an estimated K_d of 1–4 nM (Swiderska *et al.*, 2001). These authors isolated several TraM mutants that retained comparable binding affinity to TraR but, nevertheless, were unable to inhibit TraR activity, suggesting that initial binding of TraR by TraM is necessary, but not sufficient, for antiactivation.

To understand the structural basis for TraM inhibition of TraR, and the molecular mechanism of TraR–TraM interaction, we have solved the crystal structure of TraM to 1.6 Å. Our studies have revealed that TraM is a dimer that adopts a cradle-like helical bundle. Residues important for dimerization were identified and confirmed by site-directed mutagenesis studies, supporting the functional significance of homodimer formation. We also demonstrated that TraM binds to TraR with 1:1 stoichiometry. Combined with the structure of the TraR–AHL–DNA complex (Vannini *et al.*, 2002; Zhang *et al.*, 2002), our studies provide initial insights into the interface in the TraM–TraR complex and suggest an antagonistic function of TraM on TraR.

Results

Overall structure of TraM

A TraM derivative carrying an N-terminal hexahistidyl affinity tag (His₆-TraM) was crystallized, and its structure was solved by a singular anomalous dispersion

method using a preparation of His₆-TraM expressed in the presence of selenomethionine. The structure of TraM as shown in Fig. 1A is highly asymmetrical, with two long α -helices (H2, residues 26–52; and H4, residues 67–93) and two short α -helices (H1, residues 16–22; and H3, residues 55–59). Except for the first ≈ 10 residues that are not visible in the structure, the N-terminal region mainly consists of a short α -helix (H1) of seven residues. Following a tight turn, the polypeptide chain loops back with H2 arching over the intermolecular helical bundle (see below) and reverses its trajectory again, via a linker stabilized by a five-residue helix (H3), to position helix H4 such that its C-terminus is tucked between helices H1 and H2. The C-terminus of TraM is projected out as a loop. The two long α -helices (H2 and H4) twist around each other in an antiparallel topology to form a two-helix coiled-coil structure. The length of these two long coiled helices, H2 and H4 (27 and 28 residues respectively), is about 40 Å, and they traverse at an angle of $\approx 22^\circ$. As the 19-residue His-tag extension is disordered in the crystal, its effect on the interpretation of TraM structure is presumably minimal. Crystals of TraM with the His-tag extension proteolytically removed, TraM_{PC}, were also obtained but adopted a different crystal morphology and diffracted weakly to 4 Å. The role of the His₆-tag in the function and structure of TraM is minimal because our biochemical and functional experiments were carried out using both His₆-TraM and TraM_{PC} proteins in parallel, and the results were consistent.

Several orthologues of TraM exist among bacteria of the Rhizobiaceae family (Fig. 1B). Many of the residues at the key positions in the structure are either identical or functionally similar with two clusters of notably strong sequence conservation in the H2 and H4 helices.

TraM associates into a dimeric form in the crystal. Although there are two TraM molecules in the asymmetric unit, their interactions are minimal. Instead, a TraM molecule interacts extensively with its symmetric mate in the crystal lattice. Helices H1 and H4 of one TraM protomer wrap together in an antiparallel manner with their counterparts in a TraM molecule from the neighbouring asymmetric unit to form an intermolecular α -helical bundle. In this way, the two TraM monomers are bridged through a helical bundle, a structural feature commonly found in the interfaces of homodimers (Lupas, 1996). From the side view of the long helices of one TraM molecule (Fig. 1A), the structure of dimeric TraM forms the shape of a cradle with the N-terminal loop of each protein as the stands, helices H1 and H4 as the supporting walls, helix H2 as the top opening frame and helix H3 as one of the handles.

Structural variation is observed between the two TraM protomers in the asymmetric unit. The variable regions include two linkers, around the handle (H3) with the max-

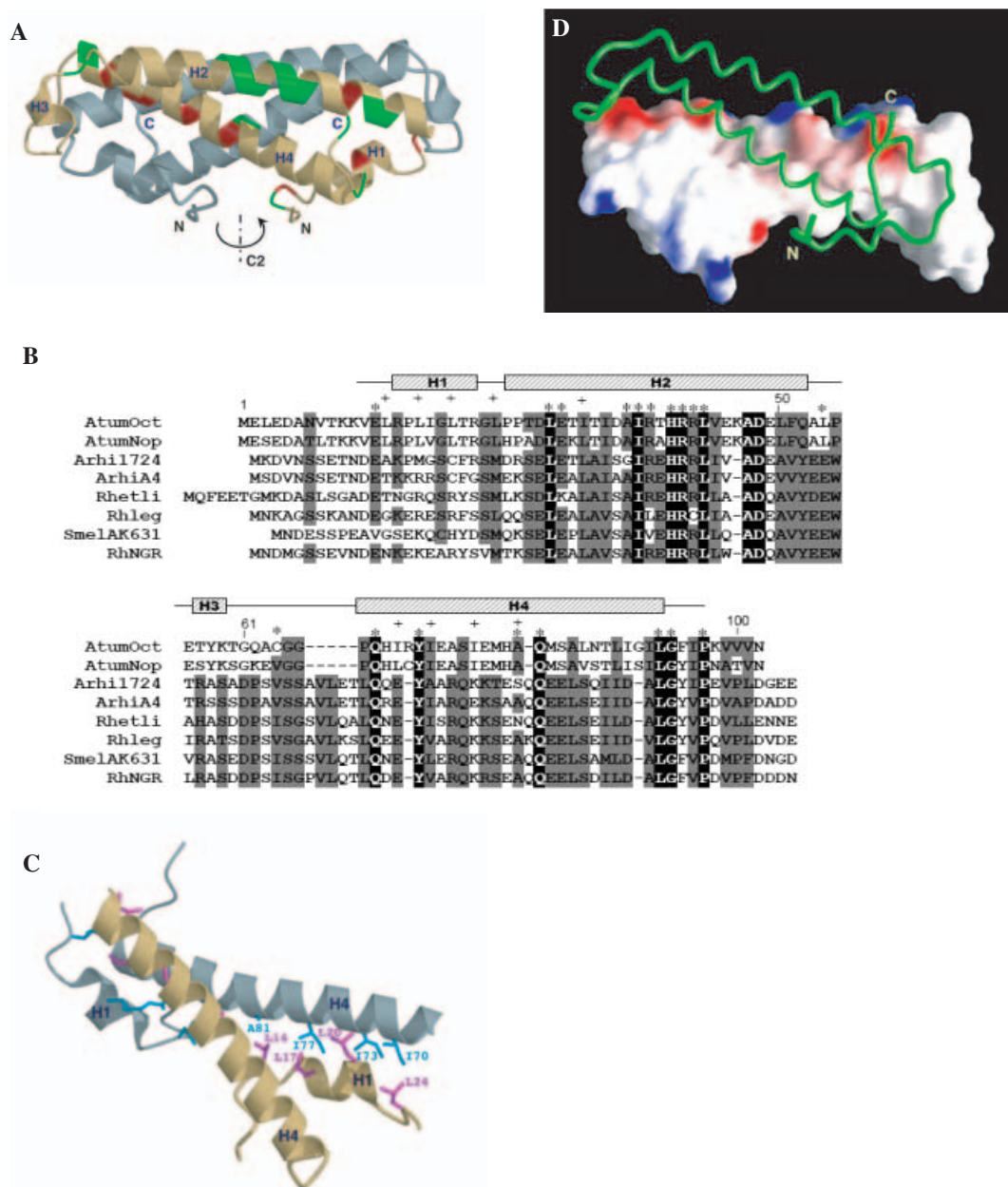


Fig. 1. Structural analysis of TraM.

A. Crystal structure of homodimeric TraM. Residues that have been mutated by Swiderska *et al.* (2001) are coloured in green and also indicated with (*) in (B), and those important for dimerization, as identified from the structure of TraM and current mutagenesis, are coloured in red and also indicated with (+) in (B). For clarity, the highlighting regions are shown in only one TraM coloured in yellow. The dimeric TraM molecules are related by a C_2 crystallographic symmetry.

B. Multiple amino acid sequence alignment of TraM proteins using CLUSTALW (Thompson *et al.*, 1994). Amino acid sequences are from the following bacteria (i) AtumOct, *A. tumefaciens* R10, the strain used in this work; (ii) AtumNop, *A. tumefaciens* C58; (iii) Arhi 1724, *A. tumefaciens* 1724; (iv) ArhiA4, *A. tumefaciens* A4; (v) Rhetli, *Rhizobium etli* CFN42; (vi) Rhleg, *R. leguminosarum*; (vii) SmelAK631, *Sinorhizobium meliloti* AK631; (viii) RhNGR, *Rhizobium* sp. NGR234. Invariant residues are highlighted in black, and structurally conserved residues are shaded in grey. Secondary structure elements are indicated above.

C. Residues involved in the dimer interface. Side-chains from one TraM molecule in yellow are coloured in magenta, and those from the other TraM in grey are in light blue. The structure is rotated to illustrate better the specific interactions within half the dimer interface, which bears a C_2 symmetry around residue A81. I32 also contributes to this Leu-rich interaction, but is omitted for clarification purpose.

D. Surface electrostatic potentials of TraM. Surface with positive potentials is coloured in red, and with negative potentials is in blue. To reveal better the hydrophobic nature of the homodimer interface within TraM, surface potentials of only one molecule are shown, while the partner is presented with the $C\alpha$ trace in green.

(A) and (C) are produced using MOLSCRIPT and RASTER 3D (Kraulis, 1991; Merritt and Bacon, 1997), and (D) is generated with GRASP (Nicholls *et al.*, 1991).

imum deviation $\approx 3 \text{ \AA}$, and the loop between H1 and H2. The C-terminal tail, the functional importance of which will be discussed later, also shows structural flexibility. On the other hand, the two long helices (H2 and H4) superimpose well with a root mean-squared deviation (r.m.s.d.) of 0.55 \AA . The overall r.m.s.d. between these two TraM protomers in the asymmetric unit is $\approx 1.1 \text{ \AA}$.

Coiled-coil structures

H4 is largely hydrophobic, conferring a unique ability to engage in forming two sets of coiled-coil structures, both intramolecular (with H2) and intermolecular (with H1 of its own and H4 of the other TraM protomer). The intramolecular coiled-coil helical structure docks the long uniformly distributed hydrophobic side of H4 against the hydrophobic side of the amphipathic helix H2. The hydrophilic side of H2 is solvent exposed and facing the top of the frame of the cradle. The regions involved in this two-helix supercoil structure follow the classical heptad repeat, in which the 'd' (the fourth) residues are hydrophobic, mostly being Leu, and the 'a' (the first) residues are non-polar or hydrophobic. In particular, we mutated L29 (a 'd' residue) and L89 (an 'a' residue) to Glu individually and found that both TraM mutant proteins became insoluble, most probably because of the destabilization of the coiled structure of H2 and H4. This extensive interhelical interaction buries a total molecular surface of 1266 \AA^2 . The two helices cross at their mid-length around His-40 (from H2) and Gln-82 (from H4). The importance of H40 and Q82 in stabilizing this supercoil structure may explain why TraM mutants with H40A and Q82A failed to inhibit TraR activity (Swiderska *et al.*, 2001).

The intermolecular coiled-coil structure includes H1 and H4 from two TraM molecules related by a twofold rotational symmetry. This intermolecular association can be divided into three regions in relation to H4. The N-terminus of H4 (I70, I73 and I77) associates intermolecularly, primarily with H1 (L14, L17, L20 and L24) and with H2 (I32) of a second TraM protomer in a leucine zipper-like manner (Fig. 1C). The centre segment of H4 makes contact with its counterpart H4 from the other TraM protomer. Finally, the C-terminus of H4 participates indirectly in this dimer interface by stabilizing its own H1, which in turn makes intermolecular contacts with H4 of the other TraM molecule. Overall, the elongated dimer interface is reinforced by two zipping interactions at both ends. A large molecular surface, $\approx 2086 \text{ \AA}^2$, most of which is hydrophobic (Fig. 1D), becomes buried as a result of dimer formation. This dimer interface is 15% larger than the estimated value (Miller *et al.*, 1987) and 74% greater than what is required to form a stable subunit association (Chothia and Janin, 1975).

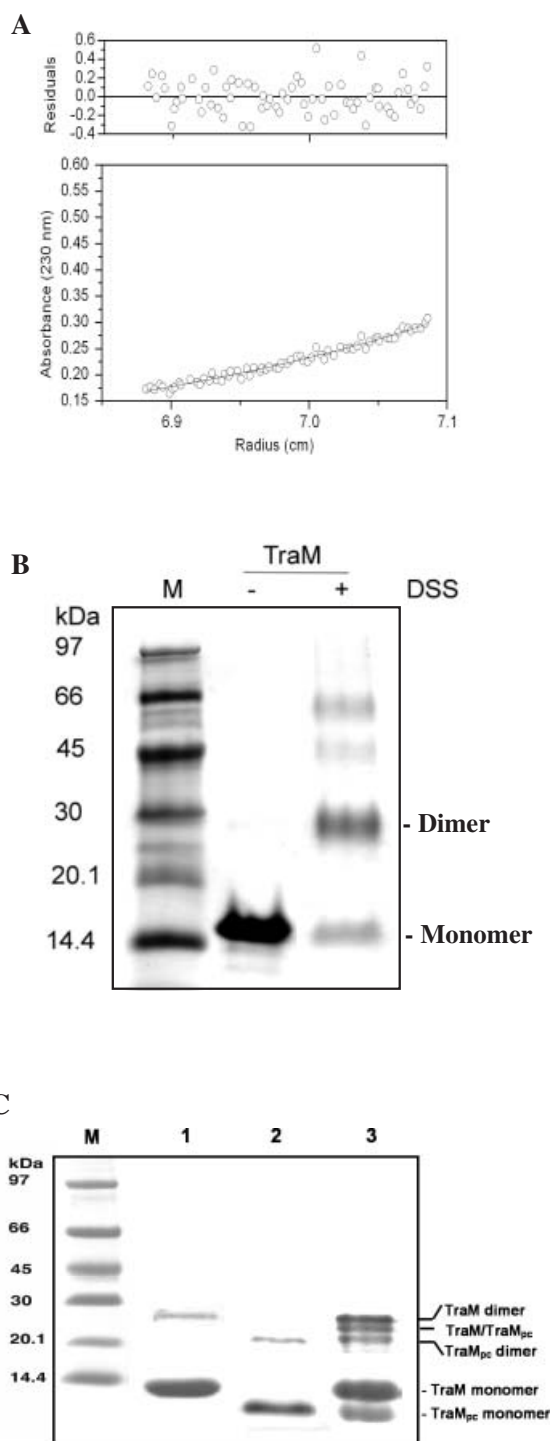
The angle between the two long helical (H4) axes is $\approx 45^\circ$, much greater than the typical $\approx 20^\circ$ inclination angle

for a coiled-coil helical structure. The enlarged crossing angle could plausibly be accounted for by the 'insertion' of H1. To examine the role of H1 in this intermolecular coiled-coil bundle, we deleted the first 20 residues of TraM, thereby disrupting the formation of H1 (16–22 amino acids). The apparent size and helical content of this TraM variant, DM21, are comparable to those of the wild-type TraM, as judged by gel filtration chromatography and circular dichroism (CD) respectively. Furthermore, DM21 inhibits TraR binding to DNA as effectively as the full length TraM (data not shown). These findings suggest that H1 or the N-terminus of TraM is functionally dispensable and plays a minimal role in maintaining the dimeric structure of TraM and perhaps TraR. It is very likely that, in the absence of H1, the two interacting helices (H4) may wrap around each other much more tightly, promoting the direct contacts and closing the inclination angle between them, yet the resulting interactive surface with TraR is still largely preserved.

TraM exists as a homodimer in solution

As expected from the extensive interactions between the two associated TraM molecules, which extend over the entire walls of the cradle structure, the dimer association is rather strong. The dimeric conformation is consistent with the observation that, in solution, TraM has an apparent molecular weight of 31.6 kDa (estimated by gel filtration chromatography), which is much higher than that of the 13.6 kDa monomeric TraM (data not shown). Considering the highly asymmetric structure of TraM revealed here, we ascribe the multimeric state of TraM to a dimer (27.2 kDa). We also carried out sedimentation equilibrium experiments (Teller, 1973) on TraM and found that, at $10 \mu\text{M}$ concentration, TraM exists predominantly as a single species with the apparent molecular weight of 27.1 kDa (Fig. 2A), in good agreement with the dimeric conformation. The goodness of this approximation is evident from the lack of scatter in the fitting residuals. Further support for the dimeric association of TraM in solution came from multiple cross-linking experiments using different cross-linking reagents. Figure 2B shows that the dimeric form is the major cross-linked product, with some tetrameric and trace amount of the trimeric forms, indicating the pre-existence of TraM dimer in solution as the predominant species. In addition, the extensive, highly stabilized dimer interaction may explain the observation that a TraM dimer is persistently observed under fully denaturing conditions (without cross-linking) on SDS-PAGE gels, even after extensive boiling of the sample (Fig. 2B).

Finally, the dimeric form of TraM disassociates in solution. When His₆-TraM (13.6 kDa, with the 19-amino-acid N-terminal His₆-tag) was incubated overnight with TraM_{PC}



(11.5 kDa, generated by proteolytic cleavage to remove a different His₆-tag extension), a new species with a molecular weight between those of homodimeric forms of TraM (27.2 kDa) and TraM_{pc} (23.0 kDa) can be visualized as shown in Fig. 2C, indicative of the formation of TraM–TraM_{pc} heterodimer (25.1 kDa). Presumably, this disassociation equilibrium between monomer and dimer con-

Fig. 2. TraM exists as a dimer in solution.

A. Sedimentation equilibrium analysis of TraM. Nine data sets were collected at 12 K, 16 K and 22 K r.p.m. and monitored at 230 nm, 234 nm and 238 nm, and were simultaneously fitted into a single species model. Shown here are a representative fit (10 μ M TraM at 12 K r.p.m. and 230 nm) and the fitting residual.

B. Cross-linking of TraM with disuccimidyl suberate (DSS). An aliquot of 10 μ l of TraM (1.5 μ g ml⁻¹) was incubated in the conjugation buffer for 2 h in the presence of DSS. For the control experiment, 25 μ l of TraM was incubated in the same conjugation buffer but without DSS. The cross-linking was quenched by 5 μ l of 1 M Tris-HCl (pH 8.0) followed by denaturing Tris-tricine PAGE. Lane M, molecular size markers.

C. Dissociation of homodimeric TraM analysed by SDS–PAGE. Equal molar amounts of diluted TraM and TraM_{pc} were incubated in 50 mM Tris-Cl, pH 8.0, 0.5 mM EDTA and 200 mM NaCl at room temperature for 12 h. The solution was concentrated before loading onto the SDS gel (lane 3). Lanes 1 and 2, typical SDS–PAGE of TraM and TraM_{pc}; M, molecular size marker.

formations of TraM is slow on account of the extensive interface within homodimeric TraM (see *Discussion*).

Directed mutagenesis of dimer interface

To confirm that the dimer structure observed in the crystal is not a fortuitous crystal packing artifact and to investigate its biological relevance, we mutated residues individually that are involved in the observed dimer interface (L14, L17, L20, L24, I32, I70, I73, I77 and A81) to Glu or Asp, with the intention of disrupting the hydrophobic interface by the introduction of charged residues. The L20E, L24E, I32E, I70E, I73E, I77E and A81D mutant proteins were found to form insoluble inclusion bodies when over-expressed in *Escherichia coli*, in contrast to the wild-type protein, which is highly soluble. These findings are consistent with predictions from the crystal structure. The ‘core’ Leu zipper-like interaction consists of residues I70, I73 and I77 of one TraM protomer with L24, I32 and L20 of a second TraM; a replacement at these positions with charged residues will severely disrupt this well-arranged hydrophobic stacking and, because of the rotational symmetry, a single drastic mutation will have at least dual effects on destabilization of the dimer interface. Residue A81, located midway along the interface, also interacts with various residues from the second TraM. A mutation to Asp will disturb the intermolecular interaction because of the charge and the steric interference. In contrast, a less drastic mutation to Ala on these residues (L20, L24, I32, I70, I73 and I77) does not affect the solubility, the apparent size (by gel filtration) and the helical content (by CD) of the resulting TraM mutant proteins (data not shown). Swiderska *et al.* (2001) showed previously that A81G had only a modest effect on TraM activity. Taken together, in the charged replacement experiments, the large mostly hydrophobic homodimer interface revealed in our structure ($\approx 1043 \text{ \AA}^2$) is exposed and most probably

leads to non-specific aggregation and therefore the formation of inclusion bodies, whereas this interface remains sequestered in the conservative Ala (Gly) mutations.

On the other hand, mutant L14E and L17E proteins are soluble, maintaining helical conformation as judged by CD and the native dimeric structure as judged by gel filtration (data not shown). These data are consistent with the observation that L14 and L17 are the residues flanking the end of the tight Leu zipper-like core; thus, the contributions of these two residues to dimer formation are modest and, as a result, the dimer interface is still largely preserved in the mutant proteins.

Binding stoichiometry in the TraM–TraR complex

The TraM–TraR complex is very stable (approximate $K_d = 1 \times 10^{-9}$ M) and migrates as an ≈ 57 kDa entity by gel filtration (Swiderska *et al.*, 2001). Both TraM and TraR exist as homodimers in solution; however, the apparent size of the TraM–TraR complex (57 kDa) is much smaller than a complex formed directly from the simple dimer–dimer interaction TraM₂–TraR₂ (80.6 kDa) and is smaller than an asymmetric complex of TraM–TraR₂ (67 kDa). The possible binding stoichiometries of the TraM–TraR complex consistent with the observed size are 2:1 (or TraM₂–TraR₁, 53.9 kDa) or 1:1 (TraM₁–TraR₁, 40.3 kDa). Here, we present evidence that supports a 1:1 binding stoichiometry in the TraM–TraR complex.

We performed *in vitro* binding assays and analysed free TraM and the TraM–TraR complex by native gel electrophoresis. TraM resolved as a rapidly migrating species on the gel (Fig. 3A). Both TraR and the TraM–TraR complex were trapped immediately upon entering the resolving gel and failed to produce a distinct band, probably because of the close approximation of their pIs (≈ 8.7 and 8.4) to the pH 8.8 of the native resolving gel. Free TraM protein was only visible in reactions in which it was in molar excess to TraR. In particular, equimolar TraR was sufficient to trap TraM into formation of the complex and resulted in a shift of the TraM position on the native gel. Next, we quantified the molar ratio within the complex by Coomassie blue-stained SDS–PAGE. The results, shown in Fig. 3B, support the model in which TraM interacts with TraR in a 1:1 molar ratio. Formation of the heterotetramer (TraM₂–TraR₂), despite its conformance to the 1:1 stoichiometry observed, is unlikely because its molecular weight is much greater than the observed value for the TraM–TraR complex (see above and Swiderska *et al.*, 2001). More importantly, we purified the TraM_{PC}–TraR complex and subjected this isolated complex to cross-linking using glutaraldehyde. As shown in Fig. 3C, a cross-linked product migrates as an ≈ 40 kDa entity in SDS–PAGE, supporting the existence of TraM_{PC1}–TraR₁ (the predicted molecular weight for TraM_{PC}–TraR is 38.2 kDa).

Lastly, we tested whether dimeric TraM is the functional species in inhibition of TraR binding to DNA by cross-linking experiments. Dimeric TraM was purified from the cross-linked reaction using gel filtration chromatography, and $\approx 80\%$ of this purified dimer was in the cross-linked conformation as estimated by SDS–PAGE (data not shown). The cross-linked TraM thus prepared was tested for its inhibitory effect on DNA binding of TraR *in vitro*. As shown in Fig. 4, the activity of this cross-linked TraM decreased dramatically to $\approx 1.6\%$ the level of the unmodified protein, suggesting that the dissociation of dimeric TraM was necessary to prevent TraR from binding to DNA. The residual blockage of TraR is most likely to be the result of the chemically unmodified TraM.

Discussion

Structural analysis reveals that the TraM quorum-sensing antiactivator forms a cradle-like dimeric structure, mainly consisting of two sets of long coiled-coil helical bundles, stabilizing the folding of both the TraM monomer and its dimer through both intra- and intermolecular hydrophobic interactions. Structure-based mutagenesis studies suggest that sequestering the extensive hydrophobic surface within the dimer interface is necessary in maintaining solubility and/or structural integrity of the TraM protein. Our biochemical analyses establish a 1:1 stoichiometry in the antiactivator TraM–TraR complex. Although current efforts are under way to determine the structure of the TraM–TraR complex, the structural data for TraM reported here, coupled with our biochemical findings, provide important insights into the interaction between TraM and TraR and the mechanistic basis of quorum-sensing control.

Dissociation of homodimers in forming the TraM–TraR complex

In the TraM₁–TraR₁ model, the TraM and TraR homodimers must dissociate to form the heterodimeric antiactivation complex. Previous studies showed that TraR exists predominantly as a homodimer in a dynamic equilibrium with its monomer (Zhu and Winans, 2001). In this study, we have shown evidence for an equilibrium between homodimer and monomer in TraM, although dissociation of the dimer is likely to be slow because of the extensive dimer interface revealed in the TraM structure. Formation of the TraM–TraR complex may rely upon the availability of monomeric TraM and TraR dissociated from their respective homodimers. Formation of the heterocomplex would therefore be dictated by the binding partner that dissociates most slowly from its homodimer, perhaps explaining the slow *in vitro* inhibition of TraR by TraM observed at equimolar concentrations (A. K. Berndtson

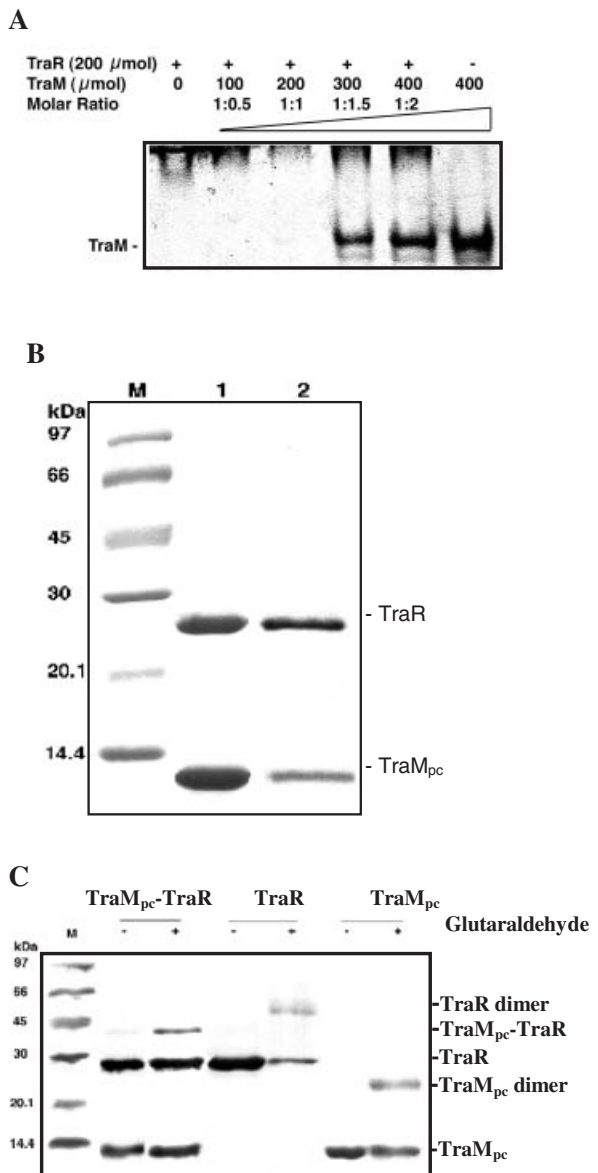


Fig. 3. The TraM–TraR antiactivator complex has 1:1 stoichiometry. **A.** Non-denaturing PAGE at pH 8.8. TraR was incubated with TraM at a range of molar ratios (TraR:TraM = 1:0.5; 1:1; 1:1.5; 1:2). Both the TraM–TraR complex and TraR alone fail to run into the resolving gel matrix. **B.** SDS–PAGE of the TraM + TraR mixture and the TraM–TraR complex. 1, TraM (90.0 μM) and TraR (21.6 μM) were mixed before loading to SDS–PAGE; 2, the TraM–TraR complex. The complex was formed in the excess amount of TraM and isolated by gel filtration chromatography. Band intensities were quantified using the Odyssey™ imaging system (LI-COR Bioscience). Ratios of band intensity/monomeric concentration for TraM and TraR were established to be 0.106 and 0.227 μM^{-1} using the TraM + TraR mixture. For the complex, the TraM band is about half as intense as that for TraR (1.1 versus 2.4); thus, the stoichiometry was calculated to be 1:1. **C.** Cross-linking of TraM_{pc}, TraR and the TraM_{pc}–TraR complex with glutaraldehyde. Samples were incubated in the presence (+) and absence (–) of 0.005% (v/v) glutaraldehyde for 1 h before loading to SDS–PAGE gel. M, molecular size markers with sizes indicated on the left.

and C. Fuqua, unpublished data). Alternatively, the TraM–TraR complex may be formed stepwise. Monomeric TraR released from its dimer may initially bind the homodimer TraM, possibly in a less specific manner, and could facilitate the disruption of dimeric TraM, displacing one TraM protomer and leading to formation of the TraM–TraR complex. Our structural and biochemical data imply a highly stable TraM dimer, and TraR-assisted disengagement of homodimeric TraM in forming the heterocomplex is energetically appealing. In a parallel situation, the antirepressor–repressor pair SinI–SinR from *Bacillus subtilis*, each existing in a higher oligomeric state, dissociate to form a tight 1:1 heterodimer (Scott *et al.*, 1999). Dimeric SinI, in rapid equilibrium with the SinI monomer, is proposed to promote dissociation of SinR homotetramer.

The homodimer interface of TraM as a potential interaction site for TraR

It is very likely that the TraM homodimer interface sequesters its TraR interaction region and may also serve as the

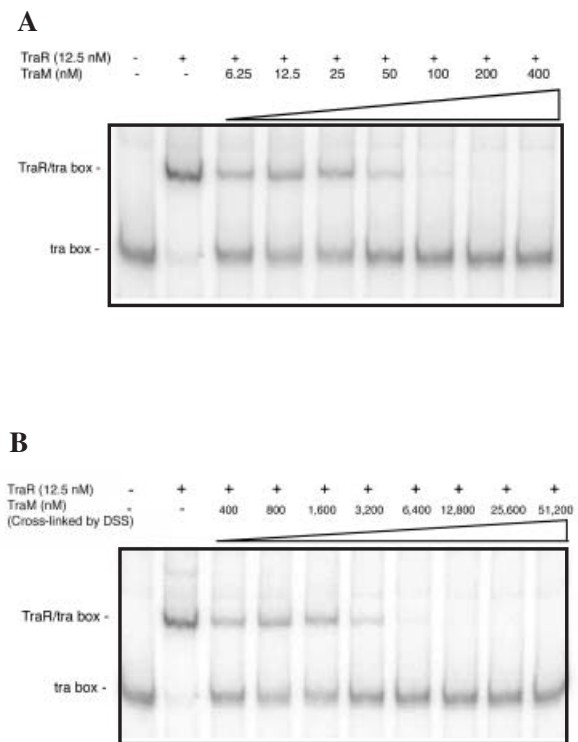


Fig. 4. The effect of cross-linking on the inhibitory activity of TraM by gel mobility assay. TraR (12.5 nM) associated with 3-oxo-C8-HSL was incubated with ^{32}P -labelled *tra* box I and either unmodified TraM (**A**) or the cross-linked TraM mixture (**B**) at the range of concentrations indicated before loading a 8% non-denaturing gel. The cross-linked mixture contains $\approx 80\%$ of the cross-linked product, with the rest being unmodified TraM. TraM inhibitory ability decreases dramatically as a result of cross-linking. While 100 nM unmodified TraM was sufficient to compete the *tra* box off TraR, it required 6400 nM linked TraM mixture to prevent TraR binding to the DNA.

TraR interaction site in the heterocomplex. This hypothesis is consistent with the inability of cross-linked TraM to inhibit TraR activity (Fig. 4), presumably because the dimer interface of cross-linked TraM is unavailable for interaction with TraR. The strategy of preserving this interface for functionality is not uncommon in macromolecular interactions. In the SinI–SinR complex, two pairs of helices, one from each protein in each pair, interact in a manner similar to the forefingers and thumbs in a handshake (Scott *et al.*, 1999). Sequences of the SinI and SinR helices are conserved between the proteins, and the conformation of the two pairs can be superimposed closely. The higher homooligomeric states of SinI and SinR may therefore use the same interface as that observed in the heterodimer SinI–SinR complex. Similarly, Lambert *et al.* (2001) found that AsiA, a multifunctional bacteriophage T4 antisyigma factor that modifies the specificity of the *E. coli* σ^{70} RNAP subunit, exists as a homodimer via a large hydrophobic interaction. The AsiA homodimer dissociates completely to form a 1:1 heterodimer with σ^{70} such that the σ^{70} -interacting region is in partial register with the AsiA dimer interface (Lambert *et al.*, 2001). For both SinR–SinI and AsiA– σ^{70} , heterodimer formation buries large areas of non-polar surface, which, if exposed, would lead to aggregation of the interacting molecules. The homodimers could function to promote protein solubility and structural integrity, and also protect the binding site for the heterodimer partner. Likewise, TraM may adopt the dimeric structure to maintain its solubility and to sequester the TraR binding site.

The involvement of a hydrophobic helical structure is common at the interacting surfaces of regulator/regulator and regulator/transcription factor complexes. For AsiA, a non-polar helix that acts as the σ^{70} binding site plays important roles in both folding of the monomer and association of homodimer (Lambert *et al.*, 2001). Likewise, the hydrophobic H4 of TraM interacts extensively with the hydrophobic side of the amphipathetic helix H2 within the monomer, while maintaining significant intimate contact with H4 (and H1) of the other subunit in the dimer. Therefore, it is plausible that, upon dimer dissociation, the newly displayed hydrophobic surface of H4 might form direct contact with TraR. Furthermore, in the structure of the homodimer TraM, large patches of hydrophobic regions are exposed throughout the structure, a substantial amount of which is contributed from H4, and these areas could potentially be immediately accessible to TraR, providing an initial interaction surface. Several mutations in the C-terminal tail of TraM, located at the end of H4, abolished binding of TraM to TraR, consistent with the importance of this helix in the TraM–TraR complex (Luo *et al.*, 2000; Swiderska *et al.*, 2001). It seems highly likely that H4 is involved in the interaction with TraR in the TraM–TraR complex.

Implications of the TraM structure on TraR antagonism

Two different inhibitors suppress quorum sensing in *A. tumefaciens* by direct interaction with TraR. TrIR shares sequence similarity with the dimerization domain of TraR (1–181 amino acids) and inhibits TraR function by forming a heterodimeric inactive TrIR–TraR complex, preventing TraR homodimer formation (Hwang *et al.*, 1999; Luo *et al.*, 2000). Although TraM has not been shown to interact with the dimerization domain of TraR, it is still conceivable that binding of TraM masks part of the dimer interface of TraR, perhaps providing steric hindrance to block docking of a second TraR protomer. In fact, based on the TraR crystal structure, helix 9 in its C-terminal domain also contributes to dimer stabilization (Vannini *et al.*, 2002; Zhang *et al.*, 2002), even though dimerization does not require helix 9 (Qin *et al.*, 2000; Chai *et al.*, 2001). An examination of N- and C-terminal portions of the TraR dimer interface revealed that the surface is largely hydrophobic (Vannini *et al.*, 2002; Zhang *et al.*, 2002). This hydrophobicity complements the non-polar characteristic of the exposed hydrophobic regions on dimeric TraM and the putative interaction region buried within the TraM dimer interface. In many protein–protein interactions, polar interactions surrounding a non-polar contact region dictate the extent of hydrophobic contact and confer binding specificity. In the SinI–SinR complex, two pairs of salt bridges, which lock two interacting helices, seal the hydrophobic interface (Scott *et al.*, 1999). In AsiA, several polar and charged residues are located at the end of the interactive surface involved in both homodimer AsiA and heterodimer AsiA– σ^{70} (Lambert *et al.*, 2001). For TraM, charged residues (mostly negative) are found at the end and along the side of H4. Patches of positive potential are located on the edge of the dimeric interface in TraR. The pairings between these complementary charge interactions might serve as determinants in docking of TraM to TraR and inhibiting TraR activity. Ultimately, details of the molecular mechanism underlying TraM–TraR interactions await structural illustration of the TraM–TraR complex.

Experimental procedures

Protein expression and purification

The coding sequence of *traM* from *A. tumefaciens* octopine-type strain R10 was cloned into pET15b (Novagen) with *NdeI* and *BamHI* sites using polymerase chain reaction (PCR). TraM with a six-histidine tag at the N-terminus separated by a Tev cleavable site was expressed in *E. coli* BL21(λ DE3) codon plus (Novagen). Cells were grown in TB medium at 37°C to an optical density at 600 nm (OD_{600}) of 1.0 and induced with 0.4 mM IPTG for 5 h. Cells were lysed at 4°C in 50 mM sodium phosphate, pH 8.0, 300 mM NaCl and 5 mM imidazole using a continuous flow microfluidizer (Microfluidics). Clear cell lysate was loaded onto a Ni-NTA

(Qiagen) column, fractionated further by Superdex75 gel filtration (Amersham Biosciences) and followed by Fast Q ion exchange chromatography (Amersham Biosciences). TraM in this work refers to the His-tag version of TraM (13.6 kDa). TraM_{PC} was generated by proteolytic cleavage of 17 out of 19 amino acids of the six-histidine tag extension by Tev protease. The final yield is 5–8 mg l⁻¹ cell culture. Selenomethionine (SeMet) TraM was prepared essentially the same as above, except that cells were grown in SeMet-containing media.

Crystallization and data collection

Crystals of H₆TraM and the SeMet derivative were obtained by hanging drop vapour diffusion at room temperature. An aliquot of 2 µl of ≈23 mg ml⁻¹ TraM was mixed with 2 µl of reservoir solution containing 0.12 M NH₄Ac, 0.06 M sodium citrate, pH 5.6, and 20% PEG2000. Crystals were stabilized in 25% glycerol plus the reservoir solution and flash frozen in liquid nitrogen. Crystals generally diffracted to >2.6 Å on a Rigaku X-ray home source. Good diffracting quality crystals were recovered for data collection at the F-2 station of Cornell High Energy Synchrotron Services (CHESS). For the native crystal, data were collected to 1.6 Å for 260°. For the SeMet crystal, diffraction data were taken in three wavelengths around the K-edge of Se, inflection, peak and remote, to 2.3 Å. These anomalous dispersion data sets were collected in 10° wedges using inverse-beam geometry before moving

to the next wavelength. (However, only the data set at the peak wavelength was used to solve the structure as it gave the best solution for the Se sites.) Crystals belong to C222 with mosaicity of 0.45°. There are two molecules per asymmetric unit, and the solvent content is 40%. Data were processed with DENZO and merged with SCALEPACK (Otwinowski and Minor, 1997).

Structure determination and refinement

Four out of eight Se sites (two for each TraM molecule) were readily identified using the anomalous data collected at the Se absorption wavelength by Shake-and-Bake (Weeks and Miller, 1999). These Se positions were then used to obtain the initial phases for the structure in SOLVE, and about 60% of the sequence was built in by RESOLVE (Terwilliger and Berendzen, 1999). Model building, using O (Jones *et al.*, 1991), was performed between rounds of structure refinement using CNS (Brunger *et al.*, 1998). Maximum likelihood using amplitudes and phase probability distribution was used as the refinement target during positional refinement and simulated annealing. The structure was refined to 2.3 Å using the diffraction data at the Se absorption wavelength, with R_{work} of 22.5% and R_{free} of 26.5%. The model was gradually refined to 1.6 Å using the native data set. The final model consists of residues from 10 to 98 for one molecule, and from 12 to 99 for the other molecule. Crystallographic data are summarized in Table 1.

Table 1. Crystallographic data.

	SeMet	Native
Unit cell dimensions (Å)		78.25 × 85.77 × 68.35
Space group		C222
Data collection		
Wavelength (Å)	0.9792 (peak)	0.9792
Resolution (Å)	15–2.3	60–1.6
Number of reflections		
Total	341 123	578 455
Unique	10 357	29 690
Redundancy ^a	14.5	9.9
Completeness (%) ^a	100 (100)	98.5 (84.8)
R _{sym} (%) ^a	12.3 (40.8)	6.1 (40.3)
I/σ ^a	24.6 (8.4)	37.4 (4.14)
Refinement statistics		
Reflections		
Working set	9822	26 178
Test set	1021	2895
R _{work} (%)	23.22 (15–2.3 Å)	20.17 (60–1.6 Å)
R _{free} (%)	26.5 (15–2.3 Å)	22.19 (60–1.6 Å)
Final model		
Non-hydrogen atoms		1351 (177 residues)
Waters		230
Average B-factors (Å ²)		
Protein		18.52
Waters		32.66
R.m.s. deviations		
Bond lengths (Å)		0.004
Bond angles (°)		1.00

R.m.s.d. is the root mean-square deviation from ideal geometry. Numbers in parentheses are for the highest resolution shell: for the SeMet data set is 2.38–2.30 Å, and for the native data set is 1.63–1.60 Å. $R_{sym} = \sum_{hkl} \sum_i |I(hkl) - \langle I(hkl) \rangle| / I(hkl)$, $R_{work} = \sum_{hkl} |F_o(hkl) - |F_c(hkl)|| / \sum_{hkl} |F_o(hkl)|$ is the crystallographic R-factor, and $R_{free} = \sum_{hkl} |F_o(hkl) - |F_c(hkl)|| / \sum_{hkl} |F_o(hkl)|$ is calculated from reflections (≈ 10% of the total reflections) and belong to a test set of randomly selected data.

a. The numbers in parenthesis refer to the last shell in the structural refinement.

CD measurements

Purified TraM proteins of $\approx 1 \text{ mg ml}^{-1}$ in 50 mM Na-phosphate buffer, pH 8.0, were subjected to CD measurements using Jasco J-715. The spectra were scaled with respect to the protein concentration, using $A_{280} = 0.297$ for TraM.

Gel mobility shift inhibition assay

Plasmid pJZ304 (Zhu and Winans, 1999) was cleaved with *Xho*I restriction endonuclease and end-labelled using [α - ^{32}P]-dCTP and the Klenow fragment of DNA polymerase I by standard techniques. Gel mobility shift assays were performed essentially as described by Swiderska *et al.* (2001). Briefly, TraR was added to a final concentration of 12.5 nM to the ^{32}P -labelled DNA in reaction buffer (12 mM Hepes-NaOH, 4 mM Tris-Cl, 60 mM potassium glutamate, 1 mM EDTA, 1 mM dithiothreitol, 12% glycerol). To assess the activity of TraM mutant proteins, a range of concentrations of purified TraM derivatives was added to the DNA-binding reactions and incubated for 2 h. The reactions were loaded directly on 8% polyacrylamide (80:1 acrylamide:bis-acrylamide) gels and separated electrophoretically. The gels were dried and analysed using a Phosphorimager (Molecular Dynamics).

Site-directed mutagenesis

Point mutations were generated using QuickChange® site-directed mutagenesis kit (Stratagene). For N-terminal deletion mutations, the desired fragments were amplified using PCR with respective primers and recloned into pET15b (Novagen) with *Nde*I and *Bam*HI sites.

Cross-linking experiments

Samples of the purified native TraM, H₆TraM or the TraM–TraR complex (15 μg) were incubated with either 100 μM disuccinimidyl suberate (DSS) or glutaraldehyde (0.005% v/v) in the conjugation buffer (50 mM Hepes, pH 7.5, 200 mM NaCl) at room temperature for 1 h. The reaction was quenched with 5 μl of 1 M Tris-Cl, pH 8.0, for 30 min. The cross-linked species were analysed on either an 8% Tris-tricine gel or a 15% SDS–PAGE gel.

Analytical ultracentrifugation

Sedimentation equilibrium experiments were carried out using a Beckman XL-A ultracentrifuge with an AN-Ti-60 rotor. TraM of 10 μM was prepared in a buffer containing 25 mM Hepes, pH 7.5, and 150 mM NaCl. Data were collected at 12 K, 16 K and 22 K r.p.m. and 25°C and scanned at 230 nm, 234 nm and 238 nm. The partial specific volume of TraM was calculated as 0.7388 $\text{cm}^3 \text{g}^{-1}$ from the amino acid sequence.

Co-ordinates

Atomic co-ordinates and structure factors have been deposited in the Protein Data Bank (accession code 1RFY).

Acknowledgements

We would like to thank Dr Y. Xiong for his generous help during structure refinement. We also thank A. Marseilles, Drs J. Ybe, K. Huffman and Q. Hao for useful discussions and timely assistance, and Drs J. Richardson and T. Donahue for critical comments on the manuscript. TraR protein was provided by Dr S. Winans at Cornell University. Data were collected at F-2 station at the Cornell High Energy Synchrotron Source (CHESS), which is supported by the National Science Foundation under award DMR 97-13424, using the Macromolecular Diffraction at CHESS (MacCHESS) facility, which is supported by award RR-01646 from the National Institutes of Health, through its National Center for Research Resources. This work was supported by an NIH grant (R01 G065260-01A1) to L.C., and NSF grants (MCB-0223724 and MCB-0238515) to C.F.

Note added in proof

During processing of this manuscript, a second group (Vanini *et al.*, 2004, *J Biol Chem*, in press) published structural data on the identical octopine-type TraM protein. The structure they report largely confirms the structure we present in our work. However, they predict a TraM₄–TraR₄ heterocomplex, in contrast to our experimental findings, which are most consistent with a TraM₁–TraR₁ complex. Resolution of these apparent differences will require further investigation.

References

- Brunger, A.T., Adams, P.D., Clore, G.M., DeLano, W.L., Gros, P., Grosse-Kunstleve, R.W., *et al.* (1998) Crystallography and NMR system: a new software suite for macromolecular structure determination. *Acta Crystallogr D Biol Crystallogr* **54**: 905–921.
- Chai, Y., Zhu, J., and Winans, S.C. (2001) TrIR, a defective TraR-like protein of *Agrobacterium tumefaciens*, blocks TraR function *in vitro* by forming inactive TrIR:TraR dimers. *Mol Microbiol* **40**: 414–421.
- Choi, S.H., and Greenberg, E.P. (1991) The C-terminal region of the *Vibrio fischeri* LuxR protein contains an inducer-independent lux gene activating domain. *Proc Natl Acad Sci USA* **88**: 11115–11119.
- Chothia, C., and Janin, J. (1975) Principles of protein-protein recognition. *Nature* **256**: 705–708.
- Dunny, G.M., and Winans, S.C. (eds) (1999) *Cell–Cell Signaling in Bacteria*. Washington, DC: American Society for Microbiology Press.
- Fuqua, C., and Greenberg, E.P. (2002) Listening in on bacteria: acyl-homoserine lactone signaling. *Nature Rev* **3**: 685–695.
- Fuqua, W.C., and Winans, S.C. (1994) A LuxR–LuxI type regulatory system activates *Agrobacterium* Ti plasmid conjugal transfer in the presence of a plant tumor metabolite. *J Bacteriol* **176**: 2796–2806.
- Fuqua, C., Burbea, M., and Winans, S.C. (1995) Activity of the *Agrobacterium* Ti plasmid conjugal transfer regulator TraR is inhibited by the product of the *traM* gene. *J Bacteriol* **177**: 1367–1373.

- Fuqua, C., Winans, S.C., and Greenberg, E.P. (1996) Consensus and consensus in bacterial ecosystems: the LuxR–LuxI family of quorum-sensing transcriptional regulators. *Annu Rev Microbiol* **50**: 727–751.
- Hwang, I., Li, P.L., Zhang, L., Piper, K.R., Cook, D.M., Tate, M.E., and Farrand, S.K. (1994) Tral, a LuxI homologue, is responsible for production of conjugation factor, the Ti plasmid *N*-acylhomoserine lactone autoinducer. *Proc Natl Acad Sci USA* **91**: 4639–4643.
- Hwang, I., Cook, D.M., and Farrand, S.K. (1995) A new regulatory element modulates homoserine lactone-mediated autoinduction of Ti plasmid conjugal transfer. *J Bacteriol* **177**: 449–458.
- Hwang, I., Smyth, A.J., Luo, Z.Q., and Farrand, S.K. (1999) Modulating quorum sensing by antiactivation: TraM interacts with TraR to inhibit activation of Ti plasmid conjugal transfer genes. *Mol Microbiol* **34**: 282–294.
- Jones, T.A., Zou, J.Y., Cowan, S.W., and Kjeldgaard, M. (1991) Improved methods for building protein models in electron density maps and the location of errors in these models. *Acta Crystallogr A* **47**: 110–119.
- Kraulis, P. (1991) MOLSCRIPT: a program to produce both detailed and schematic plots of protein structures. *J Appl Crystallogr* **24**: 946–950.
- Lambert, L.J., Schirf, V., Demeler, B., Cadene, M., and Werner, M.H. (2001) Flipping a genetic switch by subunit exchange. *EMBO J* **20**: 7149–7159.
- Luo, Z.Q., Qin, Y., and Farrand, S.K. (2000) The antiactivator TraM interferes with the autoinducer-dependent binding of TraR to DNA by interacting with the C-terminal region of the quorum-sensing activator. *J Biol Chem* **275**: 7713–7722.
- Lupas, A. (1996) Coiled coils: new structures and new functions. *Trends Biochem Sci* **21**: 375–382.
- Merritt, E.A., and Bacon, D.J. (1997) RASTER3D: photorealistic molecular graphics. *Methods Enzymol* **277**: 505–524.
- Miller, M.B., and Bassler, B.L. (2001) Quorum sensing in bacteria. *Annu Rev Microbiol* **55**: 165–199.
- Miller, S., Lesk, A.M., Janin, J., and Chothia, C. (1987) The accessible surface area and stability of oligomeric proteins. *Nature* **328**: 834–836.
- Moré, M.I., Finger, L.D., Stryker, J.L., Fuqua, C., Eberhard, A., and Winans, S.C. (1996) Enzymatic synthesis of a quorum-sensing autoinducer through use of defined substrates. *Science* **272**: 1655–1658.
- Nicholls, A., Sharp, K., and Honig, B. (1991) Protein folding and association: insights from the interfacial and thermodynamic properties of hydrocarbons. *Proteins* **11**: 281–296.
- Oger, P., Kim, K.S., Sackett, R.L., Piper, K.R., and Farrand, S.K. (1998) Octopine-type Ti plasmids code for a manopine-inducible dominant-negative allele of *traR*, the quorum-sensing activator that regulates Ti plasmid conjugal transfer. *Mol Microbiol* **27**: 277–288.
- Otwinowski, Z., and Minor, W. (1997) Processing of X-ray diffraction data collected in oscillation mode. *Methods Enzymol* **276**: 307–325.
- Parsek, M.R., and Greenberg, E.P. (2000) *Acyl*-homoserine lactone quorum sensing in gram-negative bacteria: a signaling mechanism involved in associations with higher organisms. *Proc Natl Acad Sci USA* **97**: 8789–8793.
- Qin, Y., Luo, Z.Q., Smyth, A.J., Gao, P., Beck von Bodman, S., and Farrand, S.K. (2000) Quorum-sensing signal binding results in dimerization of TraR and its release from membranes into the cytoplasm. *EMBO J* **19**: 5212–5221.
- Scott, D.J., Leejeerajumnean, S., Brannigan, J.A., Lewis, R.J., Wilkinson, A.J., and Hoggett, J.G. (1999) Quaternary re-arrangement analysed by spectral enhancement: the interaction of a sporulation repressor with its antagonist. *J Mol Biol* **293**: 997–1004.
- Swiderska, A., Berndtson, A.K., Cha, M.R., Li, L., Beaudoin, G.M., III, Zhu, J., and Fuqua, C. (2001) Inhibition of the *Agrobacterium tumefaciens* TraR quorum-sensing regulator. Interactions with the TraM anti-activator. *J Biol Chem* **276**: 49449–49458.
- Teller, D.C. (1973) Characterization of proteins by sedimentation equilibrium in the analytical ultracentrifuge. In *Methods in Enzymology*, Vol. 23. Hirs, C.H.W., and Timasheff, S.N. (eds). New York: Academic Press, pp. 346–441.
- Terwilliger, T.C., and Berendzen, J. (1999) Automated MAD and MIR structure solution. *Acta Crystallogr D* **55**: 849–861.
- Thompson, J.D., Higgins, D.G., and Gibson, T.J. (1994) CLUSTAL W: improving the sensitivity of progressive multiple sequence alignment through sequence weighting, position-specific gap penalties and weight matrix choice. *Nucleic Acids Res* **22**: 4673–4680.
- Vannini, A., Volpari, C., Gargioli, C., Muraglia, E., Cortese, R., De Francesco, R., *et al.* (2002) The crystal structure of the quorum sensing protein TraR bound to its autoinducer and target DNA. *EMBO J* **21**: 4393–4401.
- Weeks, C.M., and Miller, R. (1999) The design and implementation of SnB v2.0. *J Appl Crystallogr* **32**: 120–124.
- Williams, P. (2002) Quorum sensing: an emerging target for antibacterial chemotherapy? *Expert Opin Therap Targets* **6**: 257–274.
- Zhang, L., Murphy, P.J., Kerr, A., and Tate, M.E. (1993) *Agrobacterium* conjugation and gene regulation by *N*-acyl-L-homoserine lactones. *Nature* **362**: 446–448.
- Zhang, R.G., Pappas, T., Brace, J.L., Miller, P.C., Oulmassov, T., Molyneaux, J.M., *et al.* (2002) Structure of a bacterial quorum-sensing transcription factor complexed with pheromone and DNA. *Nature* **417**: 971–974.
- Zhu, J., and Winans, S.C. (1998) Activity of the quorum-sensing regulator TraR of *Agrobacterium tumefaciens* is inhibited by a truncated, dominant defective TraR-like protein. *Mol Microbiol* **27**: 289–297.
- Zhu, J., and Winans, S.C. (1999) Autoinducer binding by the quorum-sensing regulator TraR increases affinity for target promoters *in vitro* and decreases TraR turnover rates in whole cells. *Proc Natl Acad Sci USA* **96**: 4832–4837.
- Zhu, J., and Winans, S.C. (2001) The quorum-sensing transcriptional regulator TraR requires its cognate signaling ligand for protein folding, protease resistance, and dimerization. *Proc Natl Acad Sci USA* **98**: 1507–1512.